

Dihydroisocoumarin Derivatives from Marine-Derived Fungal Isolates and Their Anti-inflammatory Effects in Lipopolysaccharide-Induced BV2 Microglia

Dong-Cheol Kim,^{†,‡,§} Tran Hong Quang,^{†,‡,§} Nguyen Thi Thanh Ngan,^{†,‡} Chi-Su Yoon,[†] Jae Hak Sohn,[§] Jung Han Yim,[‡] Yu Feng,^{||} Yongsheng Che,[∇] Youn-Chul Kim,^{*,†} and Hyuncheol Oh^{*,†}

[†]Institute of Pharmaceutical Research and Development, College of Pharmacy, Wonkwang University, Iksan 570-749, Republic of Korea

[‡]Institute of Marine Biochemistry, Vietnam Academy of Science and Technology (VAST), 18 Hoang Quoc Viet, Cau Giay, Hanoi, Vietnam

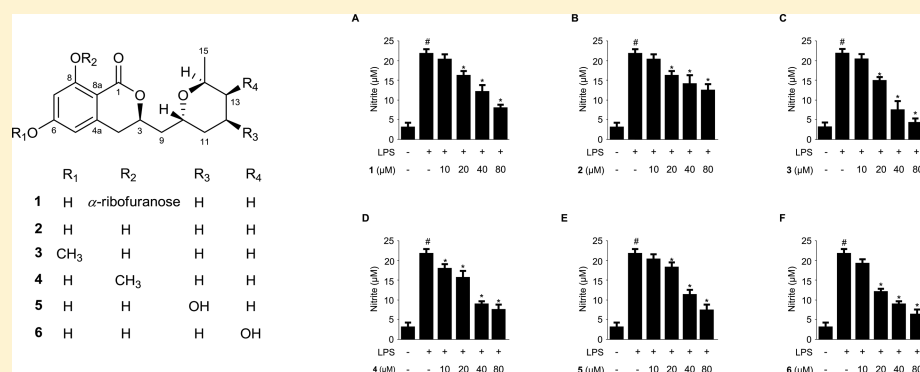
[§]College of Medical and Life Sciences, Silla University, Busan 617-736, Republic of Korea

[‡]Korea Polar Research Institute, KORDI, 7-50 Songdo-dong, Yeosu-gu, Incheon 406-840, Republic of Korea

^{||}Beijing Ditan Hospital, Capital Medical University, Beijing 100015, People's Republic of China

[∇]Beijing Institute of Pharmacology & Toxicology, Beijing 100850, People's Republic of China

Supporting Information



ABSTRACT: Chemical investigation of the EtOAc extracts of marine-derived fungal isolates *Aspergillus* sp. SF-5974 and *Aspergillus* sp. SF-5976 yielded a new dihydroisocoumarin derivative (1) and 12 known metabolites. The structures of the isolated metabolites were established by extensive spectroscopic analyses, including 1D and 2D NMR spectra and MS data. Among the metabolites, the absolute configuration of 5'-hydroxyasperentin (6) was determined by single-crystal X-ray diffraction analysis. The *in vitro* antineuroinflammatory effects of the metabolites were also evaluated in lipopolysaccharide (LPS)-stimulated microglial cells. Among the isolated metabolites, dihydroisocoumarin derivatives 1–6 (10–80 μ M) were shown to inhibit LPS-induced nitric oxide (NO) and prostaglandin E₂ (PGE₂) production by suppressing the expression of inducible NO synthase (iNOS) and cyclooxygenase-2 (COX-2), respectively, in LPS-stimulated BV2 microglia. Further, 1 (20–80 μ M) was found to suppress the phosphorylation of the inhibitor of nuclear factor kappa B- α (I κ B- α), interrupt the nuclear translocation of nuclear factor kappa B (NF- κ B), and decrease the activation of p38 mitogen-activated protein kinase (MAPK).

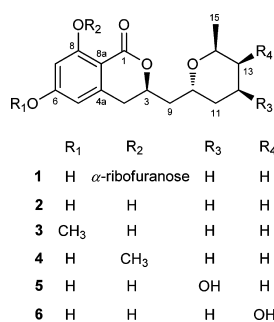
Fungi of the genus *Aspergillus*, consisting of approximately 180 recognized species, are considered rich sources of various types of bioactive fungal metabolites, including polyketides, terpenoids, peptides including diketopiperazines, alkaloids and other nitrogen-containing metabolites, shikimate derivatives, and lipids.^{1–3} In the course of our continuing search for bioactive secondary metabolites from marine-derived fungi,^{4–6} we investigated the chemical composition of extracts obtained from the cultures of two marine-derived fungal strains, *Aspergillus* spp. SF-5974 and SF-5976. As the chemical compositions of these two fungal strains were found to be

very similar, the present study describes the isolation and structural elucidation of 13 compounds, including a new dihydroisocoumarin derivative (1), from two marine-derived isolates of *Aspergillus* spp. (SF-5974 and SF-5976). Among the compounds isolated, dihydroisocoumarin-type metabolites were shown to exhibit anti-inflammatory effects in lipopolysaccharide (LPS)-stimulated BV2 microglia. Microglia are commonly regarded as brain macrophages, which are

Received: July 14, 2015

Published: December 14, 2015

activated by various stimuli. Persistent activation of microglia triggers the production of pro-inflammatory cytokines and mediators, such as tumor necrosis factor (TNF- α), interleukin 1 β (IL-1 β), nitric oxide (NO), and prostaglandins (PGs). This process is an essential feature of the inflammatory response,⁷ yet also plays a key role in the pathogenesis of neurodegenerative diseases, including stroke, Alzheimer's disease, Parkinson's disease, multiple sclerosis, and HIV-associated dementia.⁸ Thus, control of microglial activation and suppression of pro-inflammatory mediators and cytokines in activated microglia could provide therapeutic benefits in the treatment of neurodegenerative disorders. Herein, we report the isolation, structure elucidation, and antineuroinflammatory effects of fungal dihydroisocoumarins 1–6 in LPS-stimulated BV2 microglia and investigate their underlying molecular mechanism(s) of action.



RESULTS AND DISCUSSION

In the course of our search for anti-inflammatory fungal metabolites from marine-derived fungal isolates,^{14,17} the fungal strains of SF-5974 and SF-5976 were cultured on Petri plates of PDA in media containing 3% NaCl at 25 °C for 10 days. The culture plates were extracted with EtOAc, and the resultant extract was concentrated in vacuo to provide a residue. The extract obtained from SF-5976 was subjected to multiple chromatographic steps, including reversed-phase C₁₈ column chromatography, silica gel preparative TLC, and semipreparative HPLC, to give nine compounds, including six dihydroisocoumarins (1–6). Using analogous methods, 12 metabolites, including five dihydroisocoumarins (2–6), were isolated from the extract obtained from strain SF-5974. The structures of 12 known metabolites were identified as cladosporin (2),^{9,10} asperentin 6-*O*-methyl ether (3),¹¹ cladosporin 8-*O*-methyl ether (4),¹⁰ 4'-hydroxyasperentin (5),¹² 5'-hydroxyasperentin (6),¹³ neoechinulin A,¹⁴ preechinulin,¹⁵ tardioxopiperazine A,¹⁰ tardioxopiperazine B,¹⁰ flavoglucin,^{16,17} isodihydroauroglucin,¹⁶ and questinol¹⁸ by analysis of NMR, MS, and specific rotation data and comparisons with those reported in the literature. Of note, X-ray diffraction using Cu K α radiation was used to establish the previously unreported absolute configuration of 6 (Figure 1; 30% probability thermal ellipsoids).

Compound 1 was isolated as a white, amorphous powder. Its molecular formula was determined to be C₂₁H₂₈O₉ based on the ¹H and ¹³C NMR data and the observation of an [M + H]⁺ ion at *m/z* 425.1812 in its positive ion mode HRESIMS spectrum. The ¹H NMR spectrum contained signals for two *meta*-coupled aromatic protons at δ_{H} 6.56 (1H, d, *J* = 2.0 Hz, H-5) and 6.58 (1H, d, *J* = 2.0 Hz, H-7), suggesting the presence of a 1,2,3,5-tetrasubstituted benzene ring. The ¹H NMR

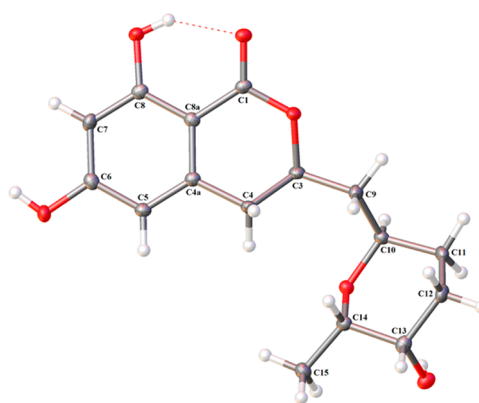


Figure 1. Thermal ellipsoid representation of 5'-hydroxyasperentin (6).

spectrum further showed signals for 10 aliphatic protons, nine oxygenated protons, including one anomeric proton at δ_{H} 5.71 (1H, d, *J* = 4.4 Hz, H-1'), and one secondary methyl group at δ_{H} 1.18 (3H, d, *J* = 6.8 Hz, H₃-15). The ¹³C NMR and DEPT spectra displayed 21 carbon signals, including one methyl, six methylenes, two sp² methines, seven sp³ methines, and five sp² nonprotonated carbons (including one sp² carbonyl carbon). The ¹³C NMR spectrum showed resonances for one lactone carbonyl carbon (δ_{C} 171.1, C-1), two oxygenated aromatic nonprotonated carbons [δ_{C} 164.9 (C-6) and 165.1 (C-8)], two aromatic nonprotonated carbons [δ_{C} 143.1 (C-4a) and 103.5 (C-8a)], and two aromatic methine carbons [δ_{C} 108.7 (C-5) and 103.6 (C-7)], suggesting that 1 contains a dihydroisocoumarin skeleton. Comparison of the ¹³C NMR data of 1 with those reported for the dihydroisocoumarin cladosporin revealed extensive similarities, except for the additional signals representing four oxymethine groups at δ_{C} 101.5 (C-1'), 73.4 (C-2'), 71.0 (C-3'), and 88.1 (C-4') and one oxymethylene group at (δ_{C} 63.1, C-5') in the ¹³C NMR spectrum of 1.^{9,10} These additional ¹³C NMR signals were assigned to a ribofuranosyl moiety by comparing the data with those of several reported furanosides, such as *O*-aryl ribofuranosides¹⁹ and isotorachryson-6-*O*- α -D-ribofuranoside.²⁰ The configuration of the anomeric position of the ribofuranose was assigned as α -configured based on the chemical shifts and coupling constant at C-1 [δ_{H} 5.71 (d, *J*_{1',2'} = 4.4 Hz) and δ_{C} 101.5] in comparison with reported values.^{19,20} However, sample limitations precluded further study of the absolute configuration of the α -ribofuranoside in 1. An HMBC correlation of δ_{H} 5.71 (H-1') with δ_{C} 165.1 (C-8) was used to locate the ribofuranosyl moiety at C-8 (Figure 2). In addition, the ¹H NMR signal corresponding to the intramolecular hydrogen bond between the 8-OH and the C-1 carbonyl oxygen in cladosporin was reported at δ_{H} 11.08, but was not found in the ¹H NMR spectrum of 1 acquired in

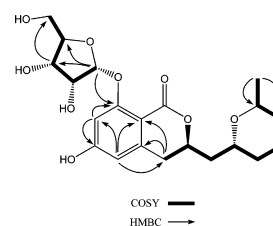


Figure 2. Selected HMBC and COSY correlations of 1.

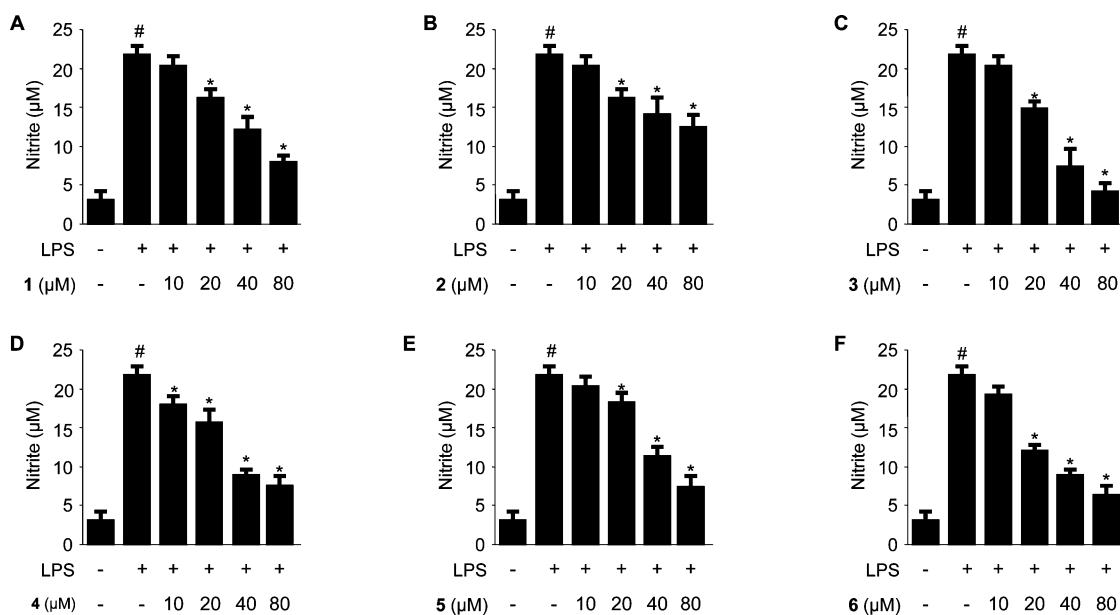


Figure 3. Effects of compounds 1–6 on nitrite (A–F) production in BV2 microglia stimulated with LPS. Cells were pretreated for 30 min with the indicated concentrations of 1–6, then stimulated for 24 h with LPS (1 $\mu\text{g}/\text{mL}$). The concentrations of nitrite were determined as described in the [Experimental Section](#). Data represent the mean values of three experiments \pm SD. [#] $p < 0.05$ vs control groups and ^{*} $p < 0.05$ compared to the group treated with LPS only.

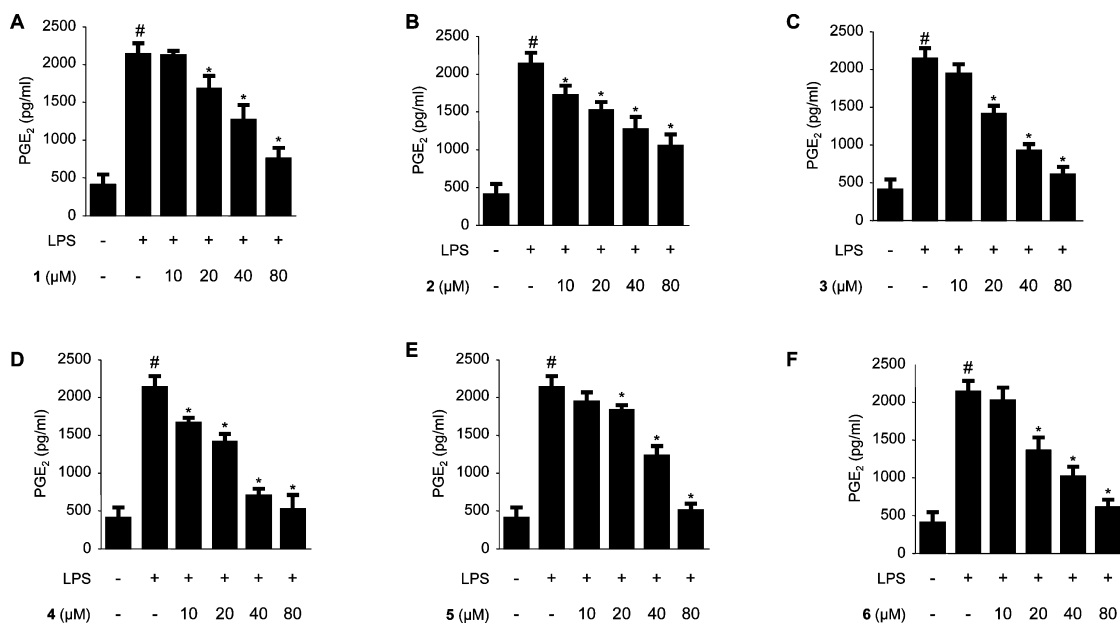


Figure 4. Effects of compounds 1–6 on PGE₂ (A–F) production in BV2 microglia stimulated with LPS. Cells were pretreated for 30 min with the indicated concentrations of 1–6, then stimulated for 24 h with LPS (1 $\mu\text{g}/\text{mL}$). The concentrations of PGE₂ were determined as described in the [Experimental Section](#). Data represent the mean values of three experiments \pm SD. [#] $p < 0.05$ vs control groups and ^{*} $p < 0.05$ compared to the group treated with LPS only.

DMSO-*d*₆ (Figure S8, [Supporting Information](#)), supporting the location of the ribofuranosyl moiety at C-8.¹⁰ The relative configuration of the remaining portion of **1** was elucidated by analysis of NOESY data and by comparison with the X-ray model of **6**. In the NOESY spectrum, H-10 showed NOE correlation with H₃-15 (δ_{H} 1.18) and H-11a (δ_{H} 1.72) but not to H-11b (δ_{H} 1.39). This observation indicated that H-10 and H-11a are located on the same side of **1**, whereas H-11b is located on the opposite side. In turn, NOE correlations of H-11b with H-13a (δ_{H} 1.67) and of H-13a with H-14 (δ_{H} 3.91) placed these protons on the same face of the tetrahydropyran

ring. On the basis of these NOESY correlations, the relative configurations at C-10 and C-14 in **1** were proposed to be the same as those in **6**. Because the absolute configuration of 5'-hydroxyasperentin (**6**) was established by X-ray diffraction analysis (Figure 1), the absolute configuration of **1** could be suggested to be 3*R*,10*R*,14*S* based on the presumed biosynthetic analogy. This assignment was also consistent with the absolute configuration of cladosporin.²¹ Ultimately, the gross structure of **1** was identified as cladosporin 8-*O*- α -ribofuranoside. The presence of an α -ribofuranosyl moiety in

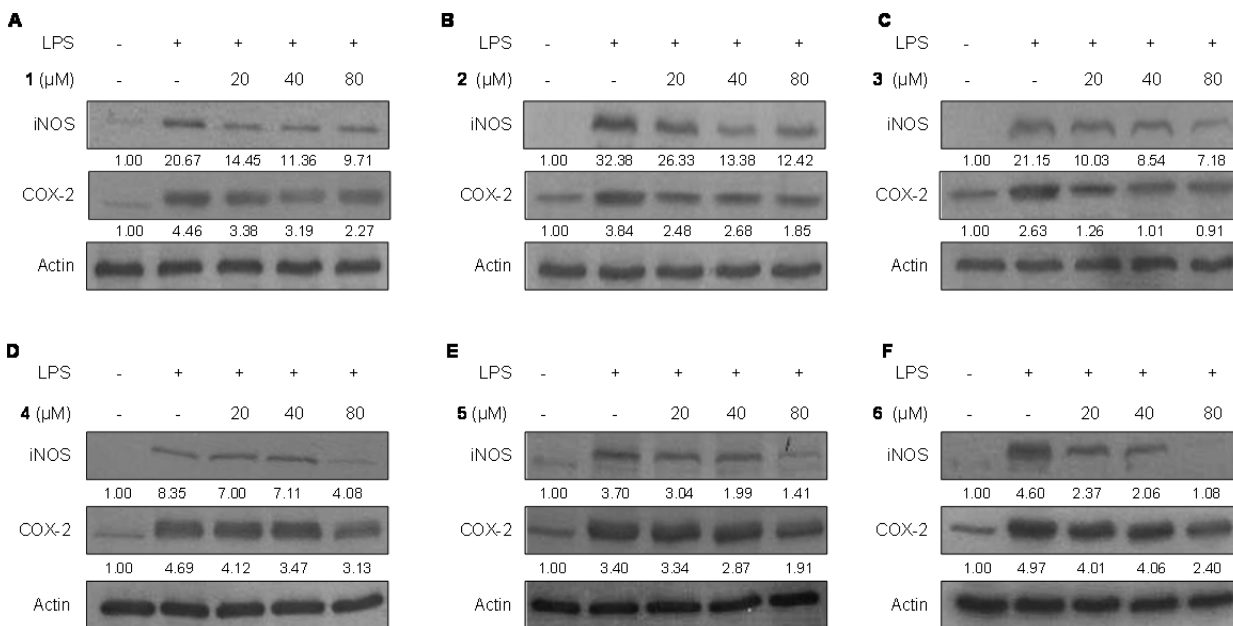


Figure 5. Effects of compounds 1–6 on protein iNOS and COX-2 expression in BV2 microglia stimulated with LPS. Cells were pretreated for 30 min with the indicated concentrations of 1–6, then stimulated for 24 h with LPS (1 μg/mL). Western blot analyses (A–F) were performed as described in the Experimental Section. Band intensity was quantified by densitometry and normalized to β-actin, and the values are presented at the bottom of each band.

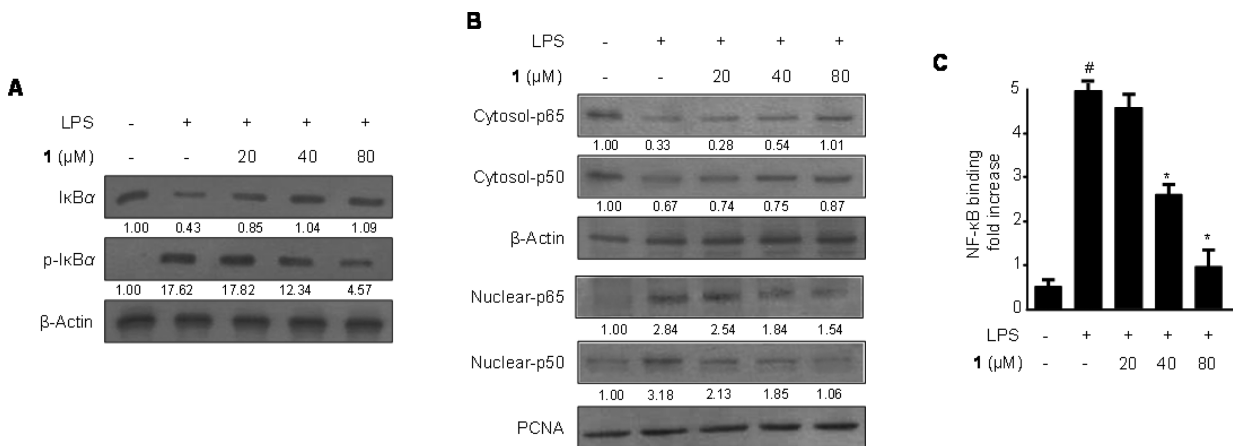


Figure 6. Effects of 1 on LPS-induced NF-κB activation in BV2 microglia. (A) Following pretreatment with 1 (20, 40, and 80 μM) for 30 min, cells were treated with LPS for 30 min. Proteins were obtained, and Western blot analysis was performed using specific IκB-α and p-IκB-α antibodies. (B) Nuclear and cytosolic extracts were isolated, and the levels of p65 and p50 in each fraction were determined by Western blot. (C) A commercially available NF-κB ELISA (Active Motif) kit was used to determine the degree of NF-κB binding in the nuclear extracts. Band intensity was quantified by densitometry and normalized to β-actin and PCNA (proliferating cell nuclear antigen). The values are presented at the bottom of each band. Relative data represent the mean values of three experiments ± SD. #*p* < 0.05 vs control and **p* < 0.05 compared to the group treated with LPS only.

the structure of 1 is noteworthy, as very few dihydroisocoumarin- α -ribofuranosides have been previously reported in nature.²²

The overproduction of pro-inflammatory mediators (e.g., NO and PGE₂) triggered by activated macrophages has been implicated in the pathology of a variety of inflammatory disorders, including sepsis and tissue damage after inflammation. Therefore, the compounds isolated from *Aspergillus* spp. SF-5974 and SF-5976 were examined for their inhibitory effects on NO and PGE₂ production in LPS-stimulated BV2 microglia. To exclude the possibility of their direct toxicity to BV2 cells, compounds 1–6 were assessed with the MTT assay. The viability of BV2 cells was not significantly affected by compounds 1–6 in the 10–80 μM range, suggesting that these compounds are not toxic to this cell line at the

concentrations tested (data not shown). Thus, for all subsequent cellular experiments, the concentrations of compounds 1–6 were kept within the range of 10–80 μM. As shown in Figure 3, treating the cells with LPS triggered an approximate 8-fold increase in nitrite concentration in the culture media, compared to that of the untreated group. However, pretreatment of the cells with compounds 1–6 for 30 min decreased the production of NO, as indicated by the nitrite concentration, in a concentration-dependent manner (IC₅₀ values of 33 ± 2; 24 ± 1; 21 ± 1; 28 ± 1; 65 ± 3, and 20 ± 1 μM, respectively). LPS treatment also triggered an approximate 6-fold increase in PGE₂ concentration in the culture media, compared to that of the untreated group. Pretreatment of the cells with compounds 1–6 for 30 min

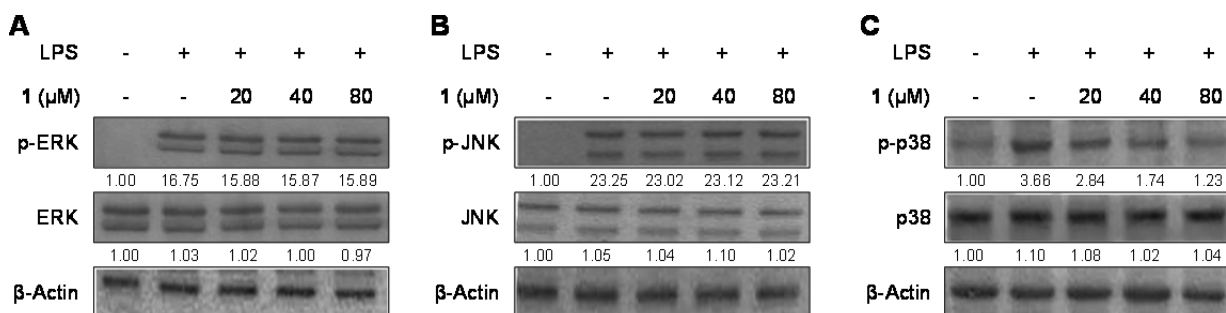


Figure 7. Effects of **1** on ERK, JNK, and p38 MAPK phosphorylation and protein expression. Cells were pretreated for 30 min with the indicated concentrations of **1** and stimulated for 30 min with LPS (1 $\mu\text{g}/\text{mL}$) (A, B, and C). The levels of (A) phosphorylated-ERK (p-ERK), (B) phosphorylated-JNK (p-JNK), and (C) phosphorylated-p38 MAPK (p-p38 MAPK) were determined by Western blotting. Representative blots from three independent experiments with similar results and densitometric evaluations are shown. Band intensity was quantified by densitometry and normalized to β -actin. The values are presented at the bottom of each band.

decreased the production of PGE_2 in a concentration-dependent manner as well (IC_{50} values of 34 ± 2 ; 27 ± 1 ; 21 ± 1 ; 30 ± 2 ; 61 ± 3 ; and $23 \pm 1 \mu\text{M}$, respectively, Figure 4). From the above results, compounds **1–6** were shown to suppress the LPS-induced production of pro-inflammatory mediators NO and PGE_2 .

Because LPS is known to induce toll-like receptor 4 (TLR-4) expression and increase the production of pro-inflammatory mediators via iNOS²³ and COX-2,^{24,25} the effects of compounds **1–6** on LPS-induced iNOS and COX-2 expression were evaluated by Western blot analysis (Figure 5). BV2 microglia were challenged with LPS (1 $\mu\text{g}/\text{mL}$) in the presence or absence of compounds **1–6** at noncytotoxic concentrations ranging from 20 to 80 μM . Each of these compounds was shown to suppress LPS-induced iNOS and COX-2 expressions in a dose-dependent manner.

NF- κB is a major transcription factor that is known to be essential for the expression of iNOS, COX-2, and inflammatory cytokines.²⁵ Therefore, to further explore the effect of dihydroisocoumarin metabolites on the NF- κB pathway, compound **1** was selected to carry out this investigation. NF- κB is composed of two subunits (p65 and p50) that are present in the cytosol as an inactive heterodimer bound to an inhibitory protein, I $\kappa\text{B-}\alpha$.²⁶ Upon stimulation by pro-inflammatory stimuli (e.g., LPS), I $\kappa\text{B-}\alpha$ is phosphorylated and proteolytically degraded, facilitating translocation of NF- κB into the nucleus to regulate target gene transcription.²⁷ Thus, it was postulated that **1** likely inhibits these pathways to suppress the production of pro-inflammatory enzymes and mediators induced by LPS. I $\kappa\text{B-}\alpha$ in macrophages was shown to be phosphorylated and degraded following LPS treatment (1 $\mu\text{g}/\text{mL}$). However, pretreatment with **1** for 30 min, at concentrations ranging from 20 to 80 μM , markedly suppressed LPS-induced phosphorylation and degradation of I $\kappa\text{B-}\alpha$ (Figure 6A), as well as p65 and p50 translocations from the cytosol to the nucleus (Figure 6B) in a dose-dependent manner. Further, pretreatment with **1** also suppressed the DNA-binding activity of NF- κB in nuclear extracts taken from the LPS-stimulated BV2 microglia. As shown in Figure 6C, stimulating the cells with LPS markedly increased the NF- κB binding activity (ca. 10-fold); however, **1** was shown to inhibit this activity in a dose-dependent manner. Therefore, it was suggested that the antineuroinflammatory effect of **1** is associated, at least in part, with the suppression of NF- κB activation.

MAPK signaling pathways also modulate the synthesis and release of pro-inflammatory mediators by activated macro-

phages during the inflammatory response.²⁸ To investigate the impact of compound **1** on the MAPK pathway, we assessed the effect of **1** on the LPS-induced phosphorylation of ERK, JNK, and p38 in BV2 microglia. As shown in Figure 7, the phosphorylation levels of ERK, JNK, and p38 were markedly increased after 30 min of stimulation with LPS. Pretreatment of the cells with **1** (20–80 μM) for 30 min significantly inhibited the LPS-induced phosphorylation of p38 in a dose-dependent manner (Figure 7C), but did not affect the phosphorylation of ERK and JNK. Neither LPS nor compound **1** was found to affect the expression of ERK, JNK, and p38 in these cells. These data suggest that compound **1** serves to regulate inflammation by inhibition of the p38 signaling pathway.

In summary, chemical investigation of the marine-derived fungi *Aspergillus* spp. SF-5974 and SF-5976 provided dihydroisocoumarin-type metabolites, including the new derivative **1**, as antineuroinflammatory constituents. Although the isolation of dihydroisocoumarin derivatives from various fungal sources has been reported, and their antibiotic and plant growth inhibitory effects are known,²⁰ the antineuroinflammatory activities of these metabolites on activated microglia have not been elucidated. In this study, dihydroisocoumarin-type fungal metabolites **1–6** were shown to inhibit the production of pro-inflammatory mediators in LPS-stimulated BV2 microglia. In addition, two major signaling pathways (NF- κB and MAPKs) activated by LPS stimulation were examined to explore the possible underlying mechanisms of the antineuroinflammatory activity of these metabolites. Our results suggest that the dihydroisocoumarins isolated from *Aspergillus* spp. SF-5974 and SF-5976 inhibit the activation of NF- κB and p38 signaling pathways in a dose-dependent manner.

EXPERIMENTAL SECTION

General Experimental Procedures. Optical rotations were recorded using a Jasco P-2000 digital polarimeter. UV spectra were recorded on a Beckman DU 800 UV–visible spectrophotometer (Beckman Coulter Inc., Fullerton, CA, USA). The FT-IR spectra were obtained using a Perkin–Elmer FT-IR spectrometer (Spectrum GX) using the KBr pellet technique. NMR spectra (1D and 2D) were recorded in CD_3OD using a JEOL JNM ECP-400 spectrometer (400 MHz for ^1H and 100 MHz for ^{13}C) or a JEOL JNM ECA-600 spectrometer (600 MHz for ^1H and 150 MHz for ^{13}C), and chemical shifts were referenced relative to the corresponding residual solvents signals (δ_{H} 4.80 and 3.30/ δ_{C} 49.0). HMQC and HMBC experiments were optimized for $^1J_{\text{CH}} = 140 \text{ Hz}$ and $^nJ_{\text{CH}} = 8 \text{ Hz}$, respectively. HRESIMS data were obtained using an ESI Q-TOF MS/MS system (AB SCIEX Triple). TLC was performed on Kieselgel 60 F₂₅₄

(1.05715; Merck) or RP-18 F_{254s} (Merck) plates. Spots were visualized by spraying with 10% aqueous H₂SO₄ solution, followed by heating. Column chromatography was performed on silica gel (Kieselgel 60, 70–230 mesh and 230–400 mesh, Merck) and YMC octadecyl-functionalized silica gel (C₁₈). HPLC separations were performed on a Synergi semipreparative C₁₈ column (21.2 × 150 mm; 4 μm particle size; 80 Å pore size, 5 mL/min). Compounds were detected by UV absorption at 210 and 254 nm.

Dulbecco's modified Eagle's medium (DMEM), fetal bovine serum (FBS), and other tissue culture reagents were purchased from Gibco BRL Co. All other chemicals were obtained from Sigma-Aldrich Co. Primary antibodies: COX-2, sc-1745; iNOS, sc-650; IκB-α, sc-371; p-IκB-α, sc-8404; p50, sc-7178; p65, sc-8008, Santa Cruz Biotechnology, p-ERK, #9101; ERK, #9102; p-JNK, #9251; JNK, #9252S; p-p38, #9211; p38:9212S, Cell Signaling Technology. Secondary antibodies: mouse, ap124p; goat, ap106p; rabbit, ap132p, Millipore. Enzyme-linked immunosorbent assay (ELISA) kits for PGE₂ were purchased from R&D Systems, Inc. (Minneapolis, MN, USA).

Fungal Material and Fermentation. *Aspergillus* sp. SF-5974 and *Aspergillus* sp. SF-5976 were isolated from an unidentified red macroalgae that were collected using a dredge at a depth of 300 m at the Ross Sea (N 76°06.256', E 169°12.675') on February 8, 2011. The surface of the red algae was sterilized, and 1 g of the sample was ground with a mortar and pestle, followed by mixing with sterile seawater (10 mL). A portion (0.1 mL) of the sample was processed utilizing the spread plate method in potato dextrose agar (PDA) medium containing sterile seawater collected in the Busan area. The plate was incubated at 25 °C for 14 days. After subculturing the isolates several times, the final pure cultures were selected and preserved at −70 °C. The fungal strains SF-5974 and SF-5976 were identified based upon analysis of their rRNA (rRNA) sequences. A GenBank search with the 28S rRNA genes of SF-5974 (GenBank accession number KJ162245) and SF-5976 (GenBank accession number KR150444) indicated *Aspergillus pseudoglaucus* (FR839678), *A. cibarius* (FR848828), and *A. glaucus* (JN938918) as the closest matches showing sequence identities of 100%. Thus, the marine-derived fungal strains SF-5974 and SF-5976 were characterized as *Aspergillus* sp. SF-5974 and *Aspergillus* sp. SF-5976, respectively, but could not be definitively identified to species.

Extraction and Isolation. The fungal strains SF-5974 and SF-5976 were cultured on 100 Petri plates (90 mm), each containing 20 mL of PDA with 3% NaCl. The plates were individually inoculated with 2 mL of seed cultures of the fungal strain and incubated at 25 °C for 10 days. Extraction of the combined agar media with EtOAc (2 L) provided an organic phase, which was then concentrated in vacuo to yield residues of SF-5974 (510 mg) and SF-5976 (629 mg). The dried extract of SF-5976 was subjected to C₁₈ flash column chromatography (5 × 26 cm), eluting with a stepwise gradient of 20, 40, 60, 80, and 100% (v/v) MeOH in H₂O (500 mL each) to give fractions 5976-1–5, respectively. Fraction 5976-3 was subjected to Sephadex LH-20 column chromatography, eluted with CH₂Cl₂–MeOH (10:1), to give six subfractions (5976-3-1–6). Subfraction 5976-3-1 was further purified using semipreparative reversed-phase HPLC, eluting with a gradient of 70–100% MeOH in H₂O over 60 min, to give neochinin A (5 mg, t_R = 15.4 min), preechinulin (1.5 mg, t_R = 17.8 min), and 1 (2 mg, t_R = 18.3 min). Fraction 5976-3-3 was separated by semipreparative reversed-phase HPLC, using a gradient of 60–100% MeOH in H₂O over 60 min, to give six subfractions (5976-3-3-1–6). Subfraction 5976-3-3-2 was further purified by preparative TLC, using hexane–EtOAc (1:15) as an eluent, to obtain 6 (8 mg, R_f = 0.6). Fraction 5976-4 was separated over Sephadex LH-20 column chromatography (CC), using CH₂Cl₂–MeOH (10:1) as an eluent, to yield two subfractions (5976-4-1 and 5976-4-2). Subfraction 5976-4-1 was further purified by silica gel preparative TLC, using CH₂Cl₂–MeOH (8:1) as an eluent, to provide 3 (2.0 mg, R_f = 0.5). Compound 2 (15 mg) was isolated from subfraction 5976-4-2 by RP C₁₈ column chromatography, using MeOH–H₂O (3:1) as an eluent. Similarly, fraction 5976-5 was subjected to Sephadex LH-20 column chromatography, eluted with CH₂Cl₂–MeOH (10:1), to provide six subfractions (5976-5-1–6). Subfraction 5976-5-3 was further separated

using RP C₁₈ column chromatography, eluted with MeOH–H₂O (4:1), to give flavoglaucin (2.5 mg) and isodihydroauroglaucin (20 mg). Using a similar method, 12 metabolites were isolated from the fungal strain SF-5974 (Supporting Information).

Cladosporin 8-O-α-ribofuranoside (1): white, amorphous powder; [α]_D¹⁶ +152 (c 0.19, MeOH); UV (MeOH) λ_{max} (log ε) 306 (2.76), 265 (3.14), 217 (3.37); IR (KBr) ν_{max} 3432, 2934, 2816, 2780, 1600, 1354, 1249, 1042, 767, 611 cm^{−1}; ¹H (CD₃OD, 600 MHz) and ¹³C NMR data (CD₃OD, 150 MHz), see Table 1; HRESIMS m/z 425.1812 [M + H]⁺ (calcd for C₂₁H₂₉O₉, 425.1812).

Table 1. ¹H and ¹³C NMR Data of Cladosporin-8-O-α-ribofuranoside (1)

| position | δ _C ^{a,b} , type | δ _H ^{a,c} (J in Hz) |
|----------|--------------------------------------|--|
| 1 | 171.1, C | |
| 3 | 77.9, CH | 4.69, m |
| 4 | 34.3, CH ₂ | 2.96, m |
| 4a | 143.1, C | |
| 5 | 108.7, CH | 6.56, d (2.0) |
| 6 | 164.9, C | |
| 7 | 103.6, CH | 6.58, d (2.0) |
| 8 | 165.1, C | |
| 8a | 103.5, C | |
| 9 | 39.1, CH ₂ | 2.13, m 1.77, m |
| 10 | 68.2, CH | 4.13, m |
| 11 | 31.4, CH ₂ | 1.72, m 1.39, m |
| 12 | 19.2, CH ₂ | 1.69, m |
| 13 | 32.7, CH ₂ | 1.67, m 1.30, m |
| 14 | 68.3, CH | 3.91, m |
| 15 | 19.9, CH ₃ | 1.18, d (6.8) |
| 1' | 101.5, CH | 5.71, d (4.4) |
| 2' | 73.4, CH | 4.20, dd (4.8, 6.0) |
| 3' | 71.0, CH | 4.10 ^d |
| 4' | 88.1, CH | 4.10 ^d |
| 5' | 63.1, CH ₂ | 3.70, dd (3.2, 12.0) 3.64, dd (3.6, 12.0) |

^aRecorded in CD₃OD. ^b100 MHz. ^c400 MHz. ^dOverlapped signals.

Cladosporin (2): white solid; [α]_D¹⁶ −20 (c 0.62, EtOH) [lit.²⁰ [α]_D²⁰ −14.0 (c 0.1, EtOH)].

X-ray Crystallographic Analysis of 6.²⁹ Upon crystallization from acetone using the vapor diffusion method, colorless crystals of 6 were obtained. A crystal (0.20 × 0.10 × 0.03 mm) was separated from the sample and mounted on a glass fiber. X-ray data were collected using the Agilent CrysAlisPro software (version 1.171.35.11) with graphite-monochromated Cu Kα radiation, λ = 1.5418 at 100(2) K. Crystal data: C₁₆H₂₀O₆, M = 308.32, space group orthorhombic, P 21 21 21; unit cell dimensions a = 7.3761(2) Å, b = 8.0325(5) Å, c = 24.6298(14) Å, V = 1459.27(13) Å³, Z = 4, D_{calcd} = 1.403 mg/m³, μ = 0.898 mm^{−1}, F(000) = 656. The structure was solved by direct methods using SHELXL-2014 and refined by using full-matrix least-squares difference Fourier techniques.³⁰ All non-hydrogen atoms were refined with anisotropic displacement parameters, and all hydrogen atoms were placed in idealized positions and refined as riding atoms with the relative isotropic parameters. Absorption corrections were performed using spherical harmonics, implemented in the SCALE3 ABSPACK scaling algorithm.³¹ The 2697 measurements yielded 2540 independent reflections after equivalent data were averaged, and Lorentz and polarization corrections were applied. The final refinement gave R₁ = 0.0347 and wR₂ = 0.0870 [I > 2σ(I)]. The Flack parameter was determined to be 0.13(11).

Cell Culture and Viability Assay. BV2 microglia cells were received from Prof. Hyun Park at College of Medicine, Wonkwang University (Iksan, Korea). The cells were maintained at 5×10^5 cells/mL in DMEM medium supplemented with 10% heat-inactivated FBS, penicillin G (100 U/mL), streptomycin (100 mg/L), and L-glutamine (2 mM) and incubated at 37 °C in a humidified atmosphere containing 5% CO₂. Cell viability was determined by adding 100 mg/mL of 3-[4,5-dimethylthiazol-2-yl]-2,5-diphenyltetrazolium bromide (MTT) to 1 mL of a cell suspension (1×10^5 cells per 1 mL in 96-well plates) and incubated for 30 min. The formazan formed was dissolved in acidic 2-propanol, and the optical density was measured at 540 nm.

Preparation of Cytosolic and Nuclear Fractions. BV2 microglia were homogenized in PER-Mammalian protein extraction buffer (1:20, w/v) (Pierce Biotechnology) containing freshly added protease inhibitor cocktail I (EMD Biosciences) and 1 mM phenylmethylsulfonylfluoride (PMSF). The cytosolic fraction of the cells was prepared by centrifugation at 16000g for 5 min at 4 °C. The nuclear and cytoplasmic cell extracts were prepared with NE-PER nuclear and cytoplasmic extraction reagents (Pierce Biotechnology), respectively.

Nitrite Production Determination.³² The nitrite concentration in the medium, an indicator of NO production, was measured with the Griess reaction. Each supernatant (100 μ L) was mixed with an equal volume of the Griess reagent (solution A, 222488; solution B, S438081; Sigma), and the absorbance of the mixture at 525 nm was determined using an ELISA plate reader.

PGE₂ Assay. BV2 microglial cells were cultured in 24-well plates, preincubated for 30 min with different concentrations of compound 1–6 and then stimulated for 24 h with LPS (Sigma-Aldrich Co.). Supernatant from the culture (100 μ L) was collected to determine the PGE₂ concentration using an ELISA kit (R & D Systems).

Western Blot Analysis.³³ BV2 microglia were harvested and pelleted by centrifugation at 16 000 rpm for 15 min. The cells were then washed with PBS and lysed with 20 mM Tris-HCl buffer (pH 7.4) containing a protease inhibitor mixture (0.1 mM PMSF, 5 mg/mL aprotinin, 5 mg/mL pepstatin A, and 1 mg/mL chymostatin). The protein concentration was determined with the Lowry protein assay kit (P5626; Sigma). An equal amount of protein from each sample was resolved using 7.5% and 12% sodium dodecyl sulfate-polyacrylamide gel electrophoresis (SDS-PAGE) and then electrophoretically transferred onto a Hybond enhanced chemiluminescence (ECL) nitrocellulose membrane (Bio-Rad). The membrane was blocked with 5% skimmed milk and sequentially incubated with the primary antibody (Santa Cruz Biotechnology) and horseradish peroxidase-conjugated secondary antibody followed by ECL detection (Amersham Pharmacia Biotech).

DNA-Binding Activity of NF- κ B. Microglia were pretreated for 3 min with the indicated concentrations of 1 and then stimulated for 30 min with LPS (1 μ g/mL). The DNA-binding activity of NF- κ B in nuclear extracts was measured using the TransAM kit (Active Motif) according to the manufacturer's instructions.

Statistical Analysis. The data are expressed as the mean \pm SD of at least three independent experiments. To compare three or more groups, one-way analysis of the variance was used, followed by Tukey's multiple comparison tests. The statistical analysis was performed with GraphPad Prism software, version 3.03 (GraphPad Software Inc.).

■ ASSOCIATED CONTENT

● Supporting Information

The Supporting Information is available free of charge on the ACS Publications website at DOI: 10.1021/acs.jnatprod.5b00614.

FT-IR, 1D and 2D NMR, and HRESI mass spectra for compound 1 (PDF) (CIF)

■ AUTHOR INFORMATION

Corresponding Authors

*E-mail: yckim@wku.ac.kr (Y.-C. Kim).

*E-mail: hoh@wonkwang.ac.kr. Fax: +82-63-852-8837. Tel: +82-63-850-6815 (H. Oh).

Author Contributions

#D.-C. Kim and T. H. Quang contributed equally to this work.

Notes

The authors declare no competing financial interest.

■ ACKNOWLEDGMENTS

This research was supported by a grant from the Ministry of Oceans and Fisheries' R&D project (PM15050).

■ REFERENCES

- (1) Bugni, T. S.; Ireland, C. M. *Nat. Prod. Rep.* **2004**, *21*, 143–163.
- (2) Rateb, M. E.; Ebel, R. *Nat. Prod. Rep.* **2011**, *28*, 290–344.
- (3) Gughani, H. C. *Front. Biosci., Landmark Ed.* **2003**, *8*, s346–357.
- (4) Quang, T. H.; Lee, D. S.; Sohn, J. H.; Kim, Y. C.; Oh, H. *Bull. Korean Chem. Soc.* **2013**, *34*, 3109–3112.
- (5) Lee, D. S.; Ko, W.; Quang, T. H.; Kim, K. S.; Sohn, J. H.; Jang, J. H.; Ahn, J. S.; Kim, Y. C.; Oh, H. *Mar. Drugs* **2013**, *11*, 4510–4526.
- (6) Quang, T. H.; Ngan, N. T.; Ko, W.; Kim, D. C.; Yoon, C. S.; Sohn, J. H.; Yim, J. H.; Kim, Y. C.; Oh, H. *Bioorg. Med. Chem. Lett.* **2014**, *24*, 5787–5791.
- (7) Fujihara, M.; Muroi, M.; Tanamoto, K.; Suzuki, T.; Azuma, H.; Ikeda, H. *Pharmacol. Ther.* **2003**, *100*, 171–194.
- (8) Brown, G. C.; Bal-Price, A. *Mol. Neurobiol.* **2003**, *27*, 325–355.
- (9) Jacyno, J. M.; Harwood, J. S.; Cutler, H. G.; Lee, M.-K. *J. Nat. Prod.* **1993**, *56*, 1397–1401.
- (10) Fujimoto, H.; Fujimaki, T.; Okuyama, E.; Yamazaki, M. *Chem. Pharm. Bull.* **1999**, *47*, 1426–1432.
- (11) Scott, P. M.; Van Walbeek, W.; MacLean, W. M. *J. Antibiot.* **1971**, *24*, 747–755.
- (12) Grove, J. F. *J. Chem. Soc., Perkin Trans. 1* **1973**, *22*, 2704–2706.
- (13) Grove, J. F. *J. Chem. Soc., Perkin Trans. 1* **1972**, *19*, 2400–2406.
- (14) Kim, K. S.; Cui, X.; Lee, D. S.; Sohn, J. H.; Yim, J. H.; Kim, Y. C.; Oh, H. *Molecules* **2013**, *18*, 13245–13259.
- (15) Wang, W. L.; Lu, Z. Y.; Tao, H. W.; Zhu, T. J.; Fang, Y. C.; Gu, Q. Q.; Zhu, W. M. *J. Nat. Prod.* **2007**, *70*, 1558–1564.
- (16) Miyake, Y.; Ito, C.; Itoigawa, M.; Osawa, T. *Biosci., Biotechnol., Biochem.* **2009**, *73*, 1323–1327.
- (17) Kim, K. S.; Cui, X.; Lee, D. S.; Ko, W.; Sohn, J. H.; Yim, J. H.; An, R. B.; Kim, Y. C.; Oh, H. *Int. J. Mol. Sci.* **2014**, *15*, 23749–23765.
- (18) Kalidhar, S. B. *Phytochemistry* **1989**, *28*, 3459–3463.
- (19) Sharma, R. K.; Singh, S.; Tiwari, R.; Mandal, D.; Olsen, C. E.; Parmar, V. S.; Parang, K.; Prasad, A. K. *Bioorg. Med. Chem.* **2012**, *20*, 6821–6830.
- (20) Du, L.; Zhu, T.; Liu, H.; Fang, Y.; Zhu, W.; Gu, Q. *J. Nat. Prod.* **2008**, *71*, 1837–1842.
- (21) Zheng, H.; Zhao, C.; Fang, B.; Jing, P.; Yang, J.; Xie, X.; She, X. *J. Org. Chem.* **2012**, *77*, 5656–5663.
- (22) Hu, Z. X.; Xue, Y. B.; Bi, X. B.; Zhang, J. W.; Luo, Z. W.; Li, X. N.; Yao, G. M.; Wang, J. P.; Zhang, Y. H. *Mar. Drugs* **2014**, *12*, 5563–5575.
- (23) Heo, S. K.; Yun, H. J.; Noh, E. K.; Park, W. H.; Park, S. D. *Immunol. Lett.* **2008**, *120*, 57–64.
- (24) Minghetti, L. *J. Neuropathol. Exp. Neurol.* **2004**, *63*, 901–910.
- (25) Kim, J. B.; Han, A. R.; Park, E. Y.; Kim, J. Y.; Cho, W.; Lee, J.; Seo, E. K.; Lee, K. T. *Biol. Pharm. Bull.* **2007**, *30*, 2345–2351.
- (26) Gomez, P. F.; Pillinger, M. H.; Attur, M.; Marjanovic, N.; Dave, M.; Park, J.; Bingham, C. O., 3rd; Al-Mussawir, H.; Abramson, S. B. *J. Immunol.* **2005**, *175*, 6924–6930.
- (27) Strayhorn, W. D.; Wadzinski, B. E. *Arch. Biochem. Biophys.* **2002**, *400*, 76–84.
- (28) Bondeson, J. *Gen. Pharmacol.* **1997**, *29*, 127–150.

(29) Crystallographic data for **6** have been deposited with the Cambridge Crystallographic Data Centre (deposition number CCDC1063985). Copies of the data can be obtained, free of charge, on application to the director, CCDC, 12 Union Road, Cambridge CB2 1EZ, U.K. (fax, +44 1223 336033; e-mail, deposit@ccdc.cam.ac.uk).

(30) Sheldrick, G. M. *Acta Crystallogr., Sect. A: Found. Crystallogr.* **2008**, *A64*, 112–122.

(31) *CrysAlisPro* Version 1.171.35.11; Oxford Diffraction Ltd.: Oxfordshire, U.K. 2011.

(32) Titheradge, M. A. *Methods Mol. Biol.* **1998**, *100*, 83–91.

(33) Li, B.; Lee, D. S.; Jeong, G. S.; Kim, Y. C. *Eur. J. Pharmacol.* **2012**, *674*, 153–162.